Seismogenic Zones in the Convergent Margin, Eastern Taiwan and Its Implications in the Luzon Forearc Deformation

Win-Bin Cheng[1,*] and Chengsung Wang[2]

ABSTRACT

Three-dimensional relocated seismicity in eastern Taiwan reveals two north-to-northeast trending seismogenic zones, one located close to the Longitudinal Valley and the other near to the crest of the Luzon arc. Earthquake focal mechanisms obtained from P-wave first motion polarity data are presented in this study for 70 events in these two seismic zones. The focal mechanism solutions for both seismic zones show mainly thrust and strike-slip faulting in the area south of 23.2°N. The horizontal projection of the events' P-axis indicates a pattern consistent with the regional NW-SE compression. However, the orientation of the events' T-axes indicates that there are different patterns for the two seismic zones. By combining evidence from seismicity, P- and T-axes, as well as detailed bathymetry, we infer that the two seismic zones (fault systems) might mark the east and west boundaries of the Luzon forearc. According to the transpressional strain model proposed in this study, the Luzon forearc represents a deforming zone, between two relatively rigid blocks, that undergoes shearing from the transcurrent component of oblique convergence in eastern Taiwan.

(Key words: Seismogenic zone, Focal mechanism, Luzon forearc)

1. INTRODUCTION

In eastern Taiwan, the Longitudinal Valley fault is considered to represent the oblique collisional boundary between the Philippine Sea plate, which carries the Luzon volcanic arc, and the Eurasian plate (Fig. 1) (e.g., Barrier and Angelier 1986; Ho 1986; Tsai 1986). Global Positioning System (GPS) measurements, collected from 1990 to 1995 (Yu et al. 1997), suggested that about 60% of the plate convergence is accommodated by deformation between the

[1]Department of Visual Communication Design, Jin-Wen Institute of Technology, Hsin-Tein, Taiwan
[2]Institute of Applied Geophysics, National Taiwan Ocean University, Taipei, Taiwan
*Corresponding author address: Dr. Win-Bin Cheng, Department of Visual Communication Design, Jin-Wen Institute of Technology, 99 Ann-Chung Road, Hsin-Tein, Taipei County, Taiwan
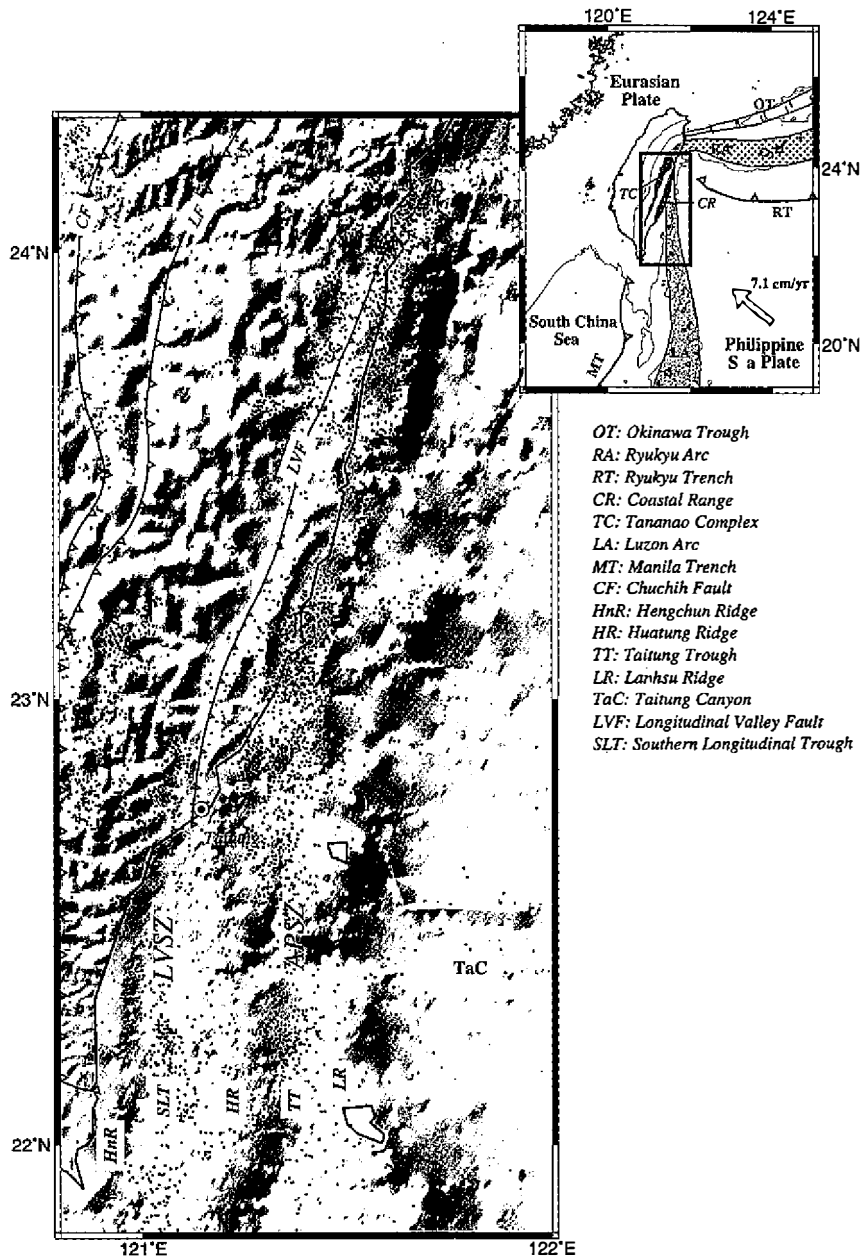E-mail: wbin@jwit.edu.tw

OT: Okinawa Trough
RA: Ryukyu Arc
RT: Ryukyu Trench
CR: Coastal Range
TC: Tananao Complex
LA: Luzon Arc
MT: Manila Trench
CF: Chuchih Fault
HnR: Hengchun Ridge
HR: Huatung Ridge
TT: Taitung Trough
LR: Lanhsu Ridge
TaC: Taitung Canyon
LVF: Longitudinal Valley Fault
SLT: Southern Longitudinal Trough

Fig. 1. Bathymetry, seismicity (solid circles), tectonic framework, and main structural unit map for eastern Taiwan. Geodynamic setting in the upper-right. Major thrust faults with open triangles on the upper side. Hypocenters of earthquakes were relocated with 3-D velocity model of Cheng et al. (1999). LVSZ: Longitudinal Valley seismic zone; APSZ: arc-parallel seismic zone

eastern flank of the Central Range and the Luzon arc (Fig. 2). It has been thought that the shortening in this region is accomplished by transfer of slip (e.g., Lundberg et al. 1997) and forearc deformation (e.g., Chemenda et al. 1997; Cheng et al. 1999). Oblique convergence also gives way to high seismicity, including the left-lateral slip observed in the northern Longitudinal Valley (Hsu 1962) and thrust events (Wu 1989; Kao et al. 1998; Kao et al. 2000). The deformation of the Luzon forearc basin is also evident in seismic reflection data (Fuh et al. 1997; Lundberg et al. 1997). A recent study on earthquake relocation and tomography of the eastern Taiwan area (Cheng et al. 1999) reported two sub-parallel seismic zones-one located close to the Longitudinal Valley and the other located west of the Luzon arc's crest (Fig. 1). However, what is the main type of faulting for these two seismic zones? Do their mechanisms vary as the collision between the Luzon volcanic arc and Taiwan increases from south to north? And, what is the relationship between the genesis of these two seismic zones and the deformation of the Luzon forearc?

Here we address these questions by studying the focal mechanisms of earthquakes of magnitude $M_L \geq 3$ and mostly shallower than 30 km, in the eastern Taiwan area. We use hypocenters relocated with three-dimensional velocity model (Cheng et al. 1999). Horizontal and depth standard errors for these events are mostly less than 2 km and 3 km, respectively. This is also the level of the largest changes caused by small changes in the model, such as whether or not station corrections are included. The events we have studied are relatively small and do not represent the total convergence in the region due to relative motion of the Philippine Sea and Eurasian plates. This will occur in large earthquakes on the major faults (e. g., 1951 Longitudinal earthquakes, M_L=7.3, 7.1, and 7.3) that are presently quiescent, a fact that is reflected in the present diffuse seismicity throughout the region. However, we believe that this type of study can give a useful insight into the present state of convergence in this area.

2. TECTONIC SETTING

Taiwan is the result of active, oblique collision between the Eurasian and Philippine Sea plates. Oblique collision has formed several mountain ranges and can be divided into two geological provinces by the Longitudinal Valley fault (Fig. 1). To the east of the fault is the Coastal Range which is mainly composed of Miocene to Pliocene andesitic volcanic units and associated flyschoid and turbidite sediments. To the west of the fault is the main body of Taiwan, distinguishable into the Central Range and the Hsüehshan Range, which is composed of a pre-Tertiary metamorphic basement overlain by Paleogene low-grade metamorphosed sediments, Neogene folded and thrusted sedimentary rock layers and Quaternary alluvial deposits (Ho 1986). The Hsüehshan Range is separated from the Central Range by the Lishan fault (LF), which branches off from the Chuchih fault (CF). The Chuchih fault is a major upthrust fault which follows the contact between the slat belt and the fold-and-thrust belt of the western foothill region (Ho 1982). The Foothill zone is a province of typical cover tectonics in which only late Tertiary and Quaternary rocks are involved (Fig. 1).

The southeastern Taiwan area is a transitional zone from a typical subduction system to the south into a collision zone to the north (Fig. 1). Based on a morphological study, Chen and
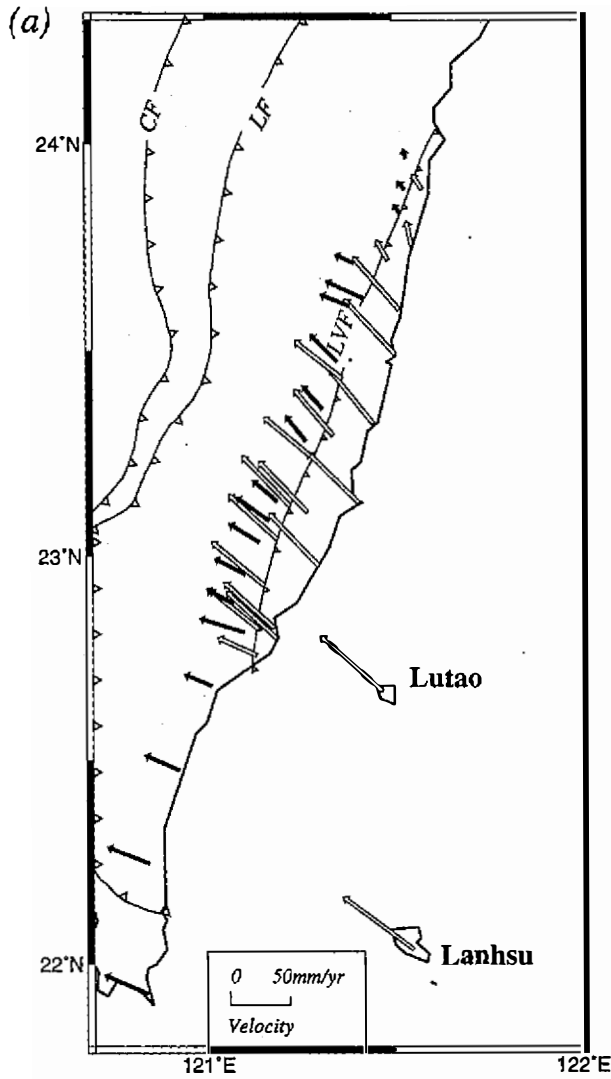
(a)

Fig. 2. (a) Velocities of GPS stations in eastern Taiwan reported by Yu et al. (1997). Black arrows indicate the velocities of the GPS stations located west of the Longitudinal Valley fault (LVF), while the white ones are stations located east of the LVF. (b) Velocities of GPS stations plotted as a function of latitude. Note that about 60% of the plate convergence is accommodated between the eastern flank of the Central Range and Luzon arc.

(b)
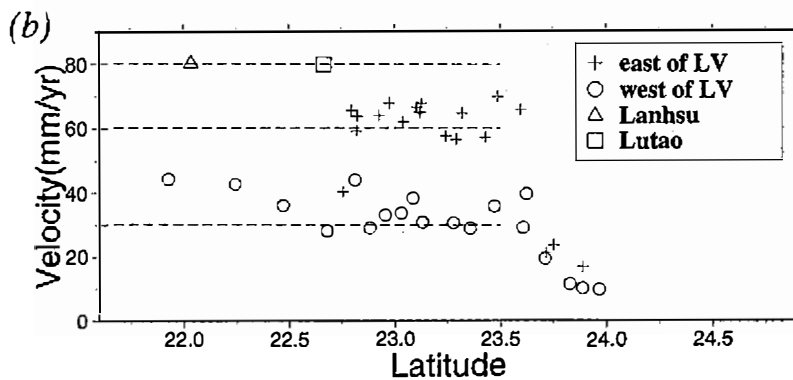
Juang (1986) divided the southeastern offshore area of Taiwan into five physiographic zones: the Hengchun Ridge, the Southern Longitudinal Trough, the Huatung Ridge, the Taitung Trough and the Lanhsu Ridge, from west to east (Fig. 1). Using magnetic and gravity data, Liu et al. (1992) indicated that the material at the basement of the Taitung Trough belongs to a volcanic arc, whereas the basements of the Southern Longitudinal Trough and Huatung Ridge do not. The Taitung Trough, the northern part of the North Luzon Trough, narrows with observable shoals toward the north and ends at the southern Coastal Range on eastern Taiwan (Page and Suppe 1981). Lutao and Lanhsu are the two northernmost islands of the Lutao-Babuyan ridge of the Luzon volcanic arc (Bowin et al. 1978). Radiometric dating shows that as you move southward along this ridge, the volcanoes are younger in this ridge belt (Richard et al. 1986). Based on magnetic basement boundary analysis, Shyu et al. (1996) also concluded that the Luzon Arc has started subsiding northward. In this part of the Luzon arc, the main volcanic activity ceased in the middle Miocene (Ho 1982, 1986). The Luzon arc presumably continues northward to include the Chimei Igneous Complex in the middle of the Coastal Range of Taiwan (Ho 1986).

3. DATA AND ANALYSIS

We study the focal mechanisms of earthquakes of magnitude M_L greater than 3.0, and mostly shallower than 30 km, in eastern Taiwan. Mechanisms have been determined for individual events using first motion polarity data. Arrival times and polarities were picked from digital seismic data recorded by the Central Weather Bureau Seismographic Network (CWBSN) during 1990 to 1998. The hypocenters were relocated with the local earthquake tomographic scheme (Thurber and Eberhart-Phillips 2000) using the three-dimensional velocity model determined for eastern Taiwan (Cheng et al. 1999). We have obtained good values of root mean square (RMS) residuals for most earthquakes analyzed.

The focal mechanism solutions were calculated with the FPFIT program (Resenberg and Oppenheimer 1985). The estimated uncertainties on strike, dip and rake of the fault-plane solutions are less than 20° and involve at least ten polarities. In order to test further the structural significance of the solutions, we selected ten of the events and analyzed them in detail. We decided to test the focal mechanisms of fixed hypocentral depths, shifting the hypocenter to 15 km and then to 1 km. In general, more stable solutions were obtained, for earthquakes where we have both good azimuthal coverage and many polarity data. Large azimuthal gaps, however, led to larger variations.

4. RESULTS

Spatial distribution of 8334 relocated hypocenters shows that there are two sub-parallel seismic groupings in eastern Taiwan-the Longitudinal Valley seismic zone (hereinafter referred to as the LVSZ) and the arc-parallel seismic zone (hereinafter referred to as the APSZ) (Fig. 1).

Figure 3 shows fault plane solutions for 70 events in eastern Taiwan. Details of the focal parameters, locations and references to these earthquakes are given in Table 1. It is clear from
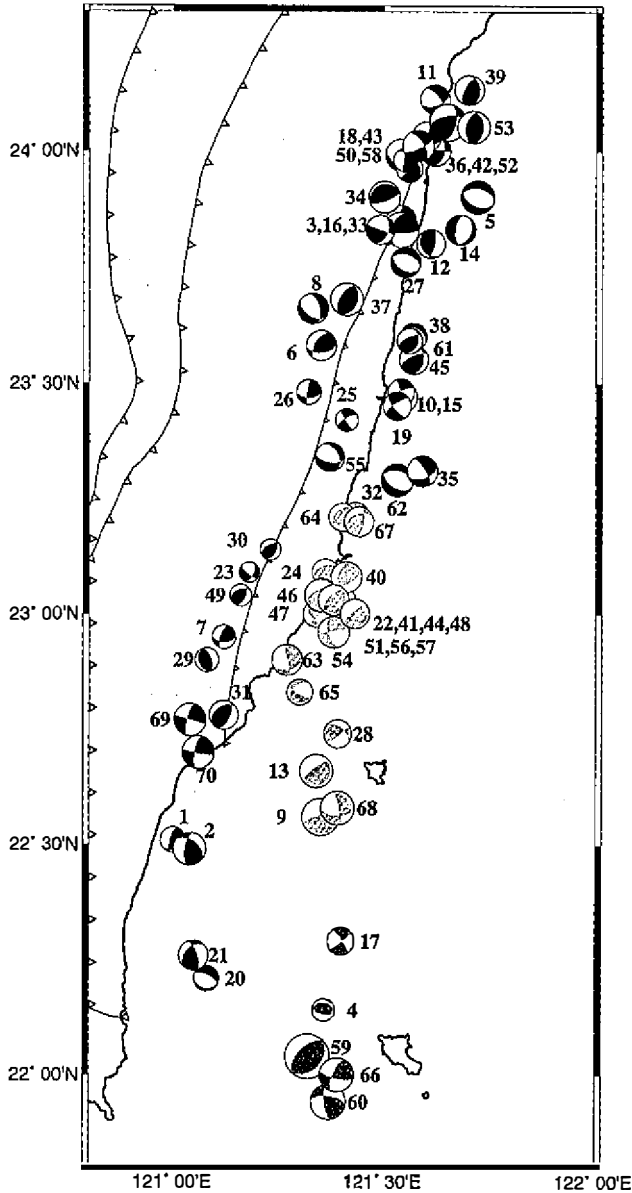
Fig. 3. Epicenters and focal mechanisms of earthquakes determined for eastern Taiwan. All equal-area projections of the lower focal hemispheres with compressional quadrants are shaded. The numbers show the event's number in Table 1. Events are from this work and other sources mentioned in the text.

Fig. 3 that the focal mechanisms of events determined in this study show a complex pattern for the APSZ and LVSZ. However, if we roughly divide these events into two groups, they predominantly show thrust (events 1, 2, 4, 9, 13, 22, 24, 29, 31, 40, 41, 44, 48, 49, and 59) and strike-slip solutions (events 21, 60, 66, 68, 69, and 70) for the APSZ and LVSZ in the area south of 23.2°N. On the other hand, there are several normal solutions observed (events 5, 8, 14, 27, 55, and 62) for both seismic zones in the area north of 23.2°N. Strike-slip solutions (events 15, 17, 19, 28, 47, 54, 63, and 65) are observed in the area between the APSZ and LVSZ.

Table 1. Summary of Source Parameters.

Letters on Fig. 3	Date[a]	Origin Time[a], UT	Lat.,[a] °N	Lon.,[a] °E	Depth[a] (Km)	Local Magnitude[a]	Plane 1 Strike deg	Dip deg	Plane 2 Strike deg	Dip deg	P Axis Azimuth deg	Plunge deg	T Axis Azimuth deg	Plunge deg	Reference[b]
1	Oct. 16, 1986	02:08	22.51	121	3	4.02	60	25	197	71	300	24	83	61	C1995
2	Nov. 29, 1986	22:50	22.49	121.04	11.51	5.16	190	65	307	46	253	11	148	52	C1995
3	Dec. 18, 1990	04:39	23.85	121.54	1.19	4.79	275	85	184	80	140	11	49	4	T
4	Feb. 4, 1991	23:17	22.14	121.36	15.77	3.52	100	55	280	35	190	10	10	80	T
5	Mar. 2, 1991	18:13	23.9	121.72	12.86	5.21	115	45	281	46	112	82	18	1	T
6	May. 7, 1991	04:36	23.58	121.35	10.2	4.74	85	50	212	54	328	2	62	61	T
7	Jun. 25, 1991	15:46	22.95	121.12	1.12	3.76	90	55	198	66	322	7	58	44	T
8	Sep. 4, 1991	12:59	23.66	121.33	13.46	4.8	125	45	344	52	316	70	56	4	T
9	Sep. 30, 1991	09:44	22.56	121.35	15.56	5.89	80	10	250	80	342	35	158	55	K2000
10	Nov. 3, 1991	04:17	23.47	121.54	40.75	5.11	55	85	147	70	103	10	9	18	T
11	Nov. 5, 1991	09:36	24.11	121.62	27.83	4.66	70	55	322	66	282	44	18	7	T
12	Nov. 20, 1991	03:19	23.8	121.61	6.16	4.51	150	30	14	67	89	20	316	63	T
13	Dec. 5, 1991	15:48	22.66	121.34	24.6	5.24	20	20	232	73	314	27	157	61	T
14	Dec. 28, 1991	21:34	23.83	121.68	9.31	4.76	20	30	188	61	83	73	282	16	T
15	Jan. 13, 1992	00:29	23.48	121.54	39.05	4.15	250	80	340	90	115	7	205	7	T
16	Apr. 19, 1992	18:32	23.83	121.54	13.72	5.55	90	75	197	42	151	20	40	45	T
17	May. 22, 1992	00:10	22.29	121.4	19.28	4.24	55	85	324	80	280	11	189	4	T
18	May. 31, 1992	13:16	23.83	121.49	20.57	4.6	20	45	290	90	345	30	235	30	T
19	Jan. 5, 1993	19:03	23.45	121.53	6.91	4.46	140	70	237	71	99	28	8	1	T
20	Mar. 5, 1993	12:56	22.21	121.08	14.54	4.04	105	25	296	65	216	70	23	20	T
21	Mar. 7, 1993	08:29	22.26	121.05	12.22	4.63	340	70	228	44	98	16	207	49	T
22	Mar. 28, 1993	09:07	23.03	121.4	30.82	4.16	25	55	222	36	122	10	261	78	T
23	Apr. 15, 1993	16:45	23.09	121.18	19.17	3.28	25	55	127	74	352	37	252	12	T
24	Jul. 2, 1993	02:39	23.09	121.36	18.23	4.16	40	45	247	48	324	2	228	77	T

Table 1. (continued)

Letters on Fig. 3	Date[a]	Origin Time[a], UT	Lat.,[a] °N	Lon.,[a] °E	Depth[a] (Km)	Local Magnitude[a]	Plane 1 Strike deg	Dip deg	Plane 2 Strike deg	Dip deg	P Azimuth deg	Axis Plunge deg	T Azimuth deg	Axis Plunge deg	Reference[b]
25	Jul. 25, 1993	03:52	23.42	121.41	19.65	3.62	240	75	147	80	103	18	194	4	T
27	Sep. 30, 1993	14:15	23.76	121.55	5.12	4.77	120	45	286	46	117	82	23	1	T
28	Nov. 13, 1993	11:18	22.74	121.39	9.52	4.36	50	80	312	51	175	19	279	35	T
29	Nov. 28, 1993	23:35	22.9	121.08	12.17	3.71	160	30	340	60	70	15	250	75	T
30	Feb. 2, 1994	19:51	23.14	121.23	13.14	3.33	25	45	244	52	316	4	216	70	T
31	May. 23, 1994	04:22	22.78	121.12	17.56	4.59	25	55	237	40	129	8	244	71	T
32	Jun. 9, 1994	14:17	23.29	121.53	40.06	5.08	120	50	285	41	82	81	203	5	T
33	Jun. 17, 1994	11:18	23.9	121.5	22.01	5.01	70	70	250	20	160	25	340	65	T
34	Jun. 30, 1994	23:45	23.99	121.54	12.44	4.99	110	40	20	90	323	33	77	33	T
35	Jul. 5, 1994	09:09	23.31	121.59	18.18	4.82	70	50	327	75	280	40	24	16	T
36	Jul. 6, 1994	21:21	23.96	121.56	7.66	4.18	45	89	315	30	288	38	162	38	T
37	Jan. 10, 1995	07:55	23.68	121.41	14.06	5.12	20	35	212	56	297	11	146	77	T
38	Jan. 28, 1995	00:38	23.6	121.57	32.05	4.19	135	55	298	36	79	78	218	10	T
39	Feb. 23, 1995	06:27	24.13	121.7	34.52	4.64	355	30	209	64	287	18	149	67	T
40	Feb. 26, 1995	08:08	23.08	121.41	22.76	4.87	60	55	195	45	129	5	27	65	T
41	Mar. 9, 1995	10:28	23	121.41	25.93	4.48	15	50	248	54	312	2	218	61	T
42	May. 1, 1995	14:50	24	121.62	12.27	4.89	275	85	11	40	334	29	220	37	T
43	May. 2, 1995	06:17	24.03	121.6	8.93	4.59	105	50	15	89	323	27	68	27	T
44	May. 9, 1995	01:03	23.01	121.37	22.61	4.9	20	40	225	53	304	7	187	75	T
45	May. 9, 1995	09:36	23.55	121.57	29.26	4.61	10	35	245	68	315	18	193	58	T
46	May. 27, 1995	18:11	23.04	121.35	22.68	5.26	10	40	227	56	300	8	188	70	T
47	May. 27, 1995	20:51	23	121.34	24.41	4.2	145	50	42	75	99	16	355	40	T
48	Jun. 6, 1995	23:21	23.04	121.35	22.91	5.06	15	45	245	57	312	7	210	62	T

Table 1. (continued)

Letters on Fig. 3	Date[a]	Origin Time[a], UT	Lat.,[a] °N	Lon.,[a] °E	Depth[a] (Km)	Local Magnitude[a]	Plane 1 Strike deg	Dip deg	Plane 2 Strike deg	Dip deg	P Axis Azimuth deg	Plunge deg	T Axis Azimuth deg	Plunge deg	Reference[b]
49	Aug. 7, 1995	16:17	23.04	121.16	17.44	3.46	25	55	250	45	136	5	238	65	T
50	Dec. 2, 1995	11:36	23.98	121.55	6.8	3.72	195	80	302	31	262	29	136	47	T
53	Dec. 20, 1995	23:56	24.05	121.71	33.74	5.06	0	40	193	51	277	6	147	81	T
54	Dec. 25, 1995	19:05	22.96	121.38	15.15	4.94	165	60	260	81	127	28	29	14	T
55	Jan. 20, 1996	04:24	23.34	121.37	19.13	4.6	100	60	329	41	321	63	211	10	T
56	Mar. 5, 1996	21:18	23.03	121.38	24.07	4.81	20	30	223	62	305	16	158	71	T
57	Apr. 10, 1996	14:14	23	121.43	19.19	4.65	40	15	230	75	318	30	144	60	K1998
58	Jun. 9, 1996	01:30	24.01	121.58	48.92	4.93	65	75	327	61	289	32	194	9	T
59	Sep. 5, 1996	23:42	22.04	121.32	9.76	7.07	45	35	225	55	135	80	315	10	T
60	Sep. 6, 1996	02:04	21.94	121.37	9.03	5.5	175	70	276	62	227	5	133	35	T
61	Sep. 12, 1996	18:25	23.59	121.56	29.72	4.01	20	35	246	64	318	16	196	63	T
62	Nov. 1, 1996	09:08	23.21	121.43	21.14	4.65	175	85	267	70	129	18	222	10	T
63	Dec. 18, 1996	02:50	22.9	121.27	11.84	4.86	80	35	350	90	290	35	50	35	T
64	Dec. 20, 1996	10:50	23.21	121.4	20.65	4.39	15	50	225	44	119	3	220	74	T
65	Jan. 8, 1997	12:14	22.83	121.3	7.29	4.06	120	75	227	42	70	45	181	20	T
66	Jan. 16, 1997	01:07	22	121.39	27.76	5.37	105	70	202	71	333	1	64	28	T
67	Feb. 13, 1997	08:29	23.2	121.44	21.82	4.69	10	65	253	46	128	11	232	52	T
68	Oct. 22, 1997	11:16	22.58	121.39	20.18	5.3	85	50	349	82	299	34	44	21	T
69	Jan. 18, 1998	19:56	22.77	121.04	2.61	5.07	195	75	105	89	151	11	59	11	T
70	Jan. 20, 1998	23:29	22.7	121.06	5.49	5.07	100	85	192	70	148	10	54	18	T

[a] Event dates, epicenters (Lat., latitude; Lon., longitude), local magnitudes are those reported by the Central Weather Bureau.

[b] Cited reference. C1995 (Cheng 1995); K1996 (Kao et al. 1998); K2000 (Kao et al. 2000); T (This study).

The P- and T-axes for all the mechanisms mentioned above in eastern Taiwan are shown in Fig. 4 and Table 1. Compilation of Fig. 4 has involved specifying which of the nodal planes in each solution was the fault plane and needs some justification. In case of almost pure dip-slip faulting (such as events 9, 13, and 34) the direction is insensitive to the choice of fault plane. Some choices were made because the earthquake occurred close to known active or historical surface faulting (events 30, 31, and 37) or were associated with topography that make the choice more likely (events 7, 23, 29, 49, 69, and 70). Apart from three events (events 4, 20, and 28), the pattern for the region shows mainly NW-SE trending (Fig. 3). Similarly, there is broad clustering towards near-horizontal NE-SW extension. However, the APSZ shows T-axis directions that are quite distinct from the horizontal ones found in the LVSZ. A depth section in the E-W direction of the P- and T-axes of the events located south of 23.2°N is shown in Fig. 5.

5. DISCUSSION

As shown in the earthquake focal mechanisms (Fig. 3), frequent seismicity (Fig. 1), and GPS observations (Fig. 2), the eastern Taiwan collision zone is characterized by strong compression oriented approximately perpendicular to the major structural trend of the Luzon arc. Oblique plate-convergence would also produce arc-parallel gradients in the horizontal shear stress on plate-boundary faults, that in turn results in arc-parallel stretching or compression of the forearc (McCaffrey 1992). For example, GPS measurements (Fig. 2b) indicate that the velocities of Lutao and Lanhsu are larger than those of other stations to the east of Longitudinal Valley and are in the order of about 20 mm/yr. In other words, part of the plate convergence is accommodated by deformation between the eastern flank of the Central Range and the Luzon arc, i.e., the Luzon forearc area. In fact, previous studies (e.g., Dahlen et al. 1984; Byrne and Fisher 1990; Shyu et al. 1996; Kao et al. 2000), have noted that the forearc basin and the accretionary prism located to the west of the Luzon arc are of low strength and can deform easily in response to plate convergence. However, the deformation pattern, and its boundaries, for the closing Luzon forearc are relatively unknown.

5.1 Significance of the Longitudinal Valley and Arc-Parallel Seismic Zones

The oblique collision between the Luzon arc and continental shelf started near the Hualien area about 4 million years ago, and moved progressively southward to reach Taitung about 1 million years ago (Lee et al. 1991). The spacing between the Luzon arc and Taiwan, measured from Lutao to the Longitudinal Valley, is about 50 km and decreases northwards (Fig. 1). In a modern arc-trench system, the minimum distance of the spacing between arc and trench is about 100 km. If the Longitudinal Valley represents an ancient trench, the closing between the Luzon arc and Longitudinal Valley implies that most of the forearc block has been shortened or plunged into the mantle (e.g., Cheng et al. 1999; Malavieille et al. 1999).

The stress regime of the LVSZ and APSZ, as inferred from the earthquake strain axes, appears to be dominated by subhorizontal compression (Fig. 4a and Table 1). In general, the P-axes of events in the APSZ and LVSZ show an orientation of 300° ±30°. This is indistin-
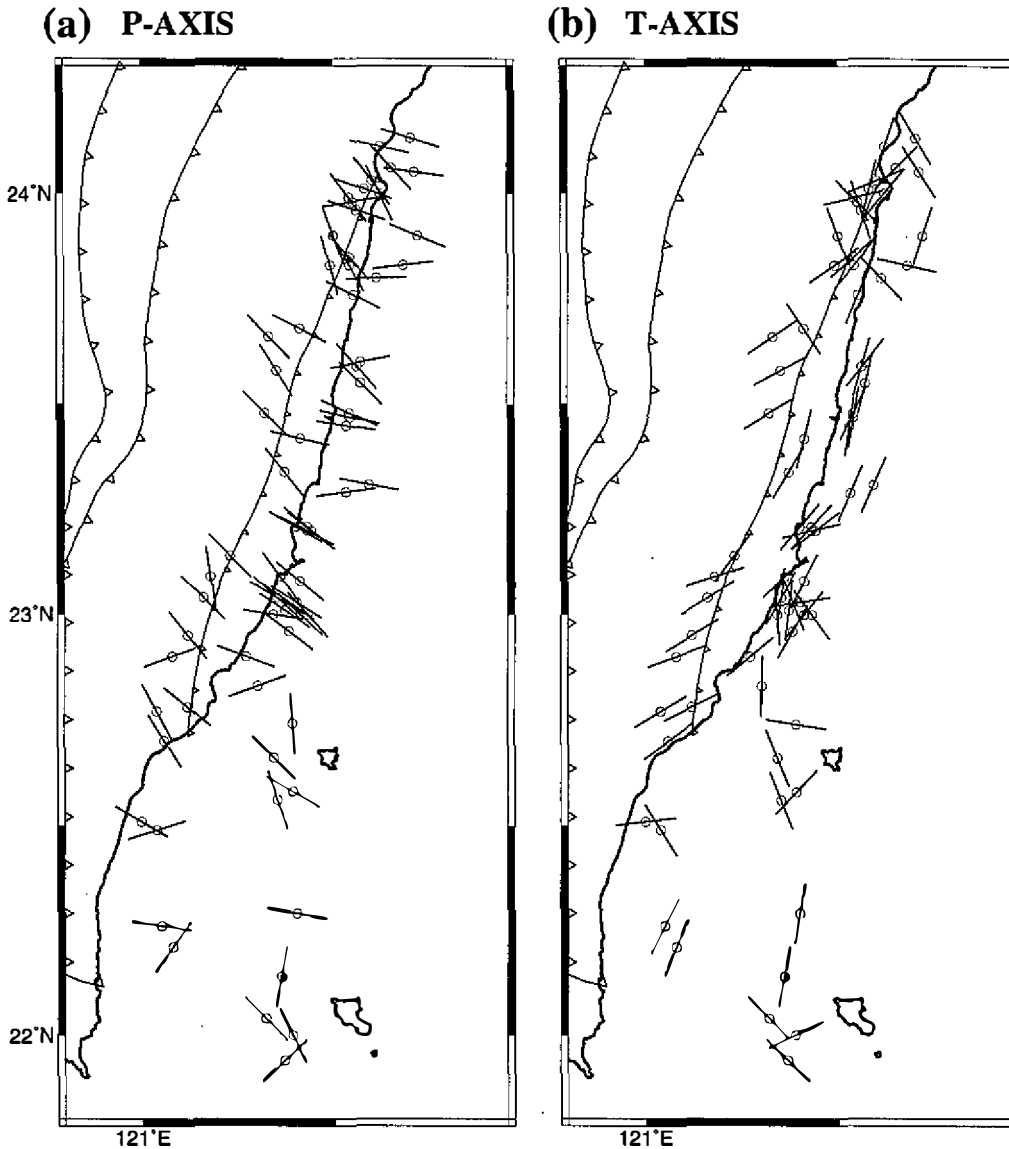
(a) P-AXIS

(b) T-AXIS

Fig. 4. Map of horizontal projections and locations of the P- (left) and T- (right) axes for earthquakes shown in Fig. 3. Details are the same as for Fig. 3 and Table 1.

guishable from the average P-axis azimuth of 295° and 297° for the region north and south of 23°, respectively, determined by Kao et al. (2000). It is also consistent with the azimuth of the axes of maximum relative shortening in eastern Taiwan determined geodetically (Yu et al. 1997). In addition, low-angle thrusting mechanisms near the plate interface, indicative of strike-slip motion between the plates, do not extend deeper (Fig. 5). On the other hand, the orienta-

(a) P-axes
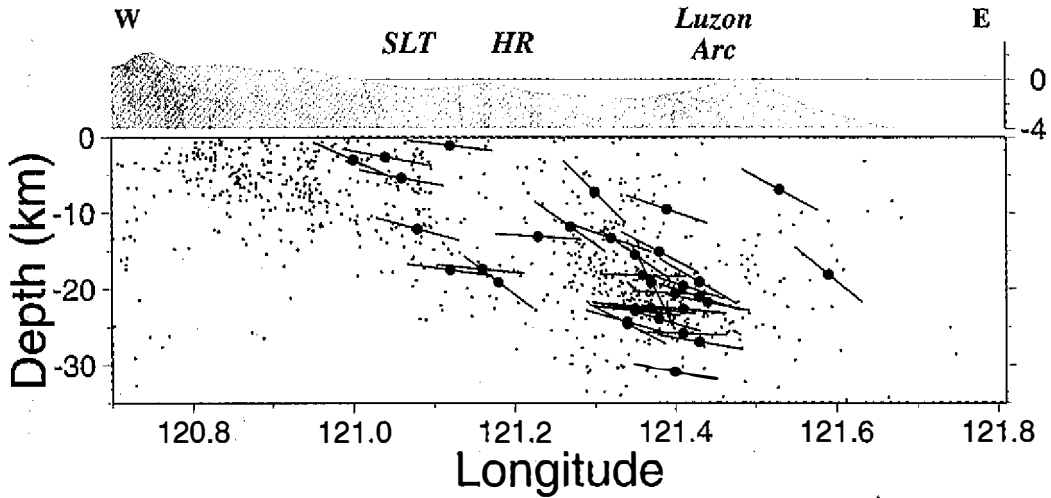
(b) T-axes
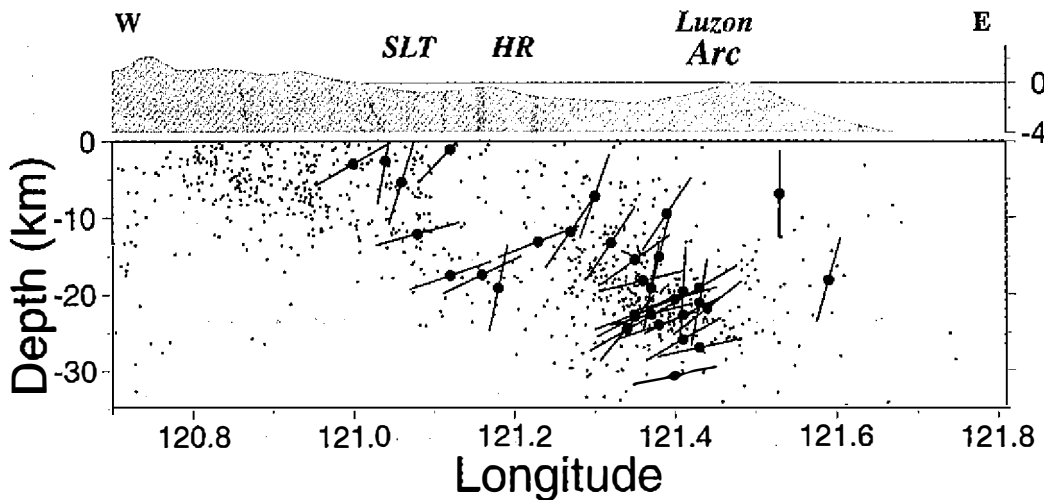
Fig. 5. Depth section of the seismiogenic zones in eastern Taiwan, together with projections of the P- and T-axes for the events located south of 23.2°N determined in this study. HR: Hengchun Ridge; SLT: Southern Longitudinal Trough. Solid dots represent hypocenters of earthquakes relocated with 3-D velocity model.

tion of the T-axes indicates that there are different patterns for the APSZ and LVSZ in eastern Taiwan. The T-axes clustered in the azimuth, average 234° ±20° for the LVSZ events, and 190° ±30° for the APSZ events. The average azimuth of the T-axes of events in the APSZ is rotated some 44° anticlockwise out of the average azimuth of the LVSZ.

By combining evidence from seismicity (Figs. 1 and 3, and Table 1), P- and T-axes (Figs. 4 and 5) and detailed bathymetry, we infer that the development of the APSZ and LVSZ has important tectonic implication. Our study suggests that both might mark obvious east and west boundaries of the Luzon forearc. It has been proposed that for high angles of oblique plate convergence, the thrust wedge will move laterally relative to the underthrust slab and separates from the upper plate by a strike-slip fault, defining a forearc sliver (e.g., Platt 1993). Although the plate-convergence angle between the Eurasian and Philippine Sea plates is larger than 60° if the Longitudinal Valley plays as a plate interface, we can regard the APSZ as one component accommodating the transfer of oblique slip. This is physically reasonable because the more the Luzon forearc sliver is indenting the Eurasian continental margin, the higher resistance against the forearc sliver expected. This also probably explains why the seismicity of the APSZ is more active than that of the LVSZ (Fig. 1).

5.2 Luzon Forearc Deformation

Figure 3 indicates that several moderate strike-slip events (events 17, 28, 60, 66, and 68) occurred in the APSZ in the area south of 23.2° (Fig. 3). In this region, the oblique convergence between Philippine Sea and Eurasian plates might have been partitioned into shortening in the Luzon forearc and right-lateral strike-slip in eastern Taiwan. However, the partitioning is not perfect, as the complex pattern of focal mechanisms north of about 23.2°N shows. Because the right-lateral strike-slip motion in eastern Taiwan might be accommodated by seismic slip on the major Longitudinal Valley faults, the Luzon forearc must be deforming mostly aseismically, either by creeps on faults or by folding as revealed in seismic reflection data (Fuh et al. 1997; Lundberg et al. 1997). Therefore, it might be expected that the shear strength of the Luzon forearc is relatively small, such that the deformation and large strike-slip fault in the forearc would take place due to the lateral component of the relative plate convergence. Many low-angle thrust events lie within the dipping seismic zone (Fig. 5) and thus represent the deformation of the forearc area.

As mentioned above, the Luzon forearc is located between the Luzon arc and Central Range in eastern Taiwan. The seismological data presented in this paper confirm that the Luzon forearc is undergoing a marked tectonic evolution and provides further evidence of active compression along its external front, as shown in Fig. 3. We propose that the obliquity of the plate convergence vector resulted in (1) a stress field with NE-SW extension, (2) generation of NW-SE fractures, and (3) sinistral shear along the LVSZ and APSZ. Figure 6 is not intended as a realistic sketch of the tectonic evolution of the region, but merely as an illustration of the sort of processes that might occur. This model is based on focal mechanisms, seismicity, as well as geodetic, geological, and topographic data. Given the Luzon arc trend of 5°, a convergence rate of 7 cm/yr, and total partitioning of the strike-slip component of the plate slip vector (310°) into the Luzon arc, this tectonic setting likely resulted in sinistral slip
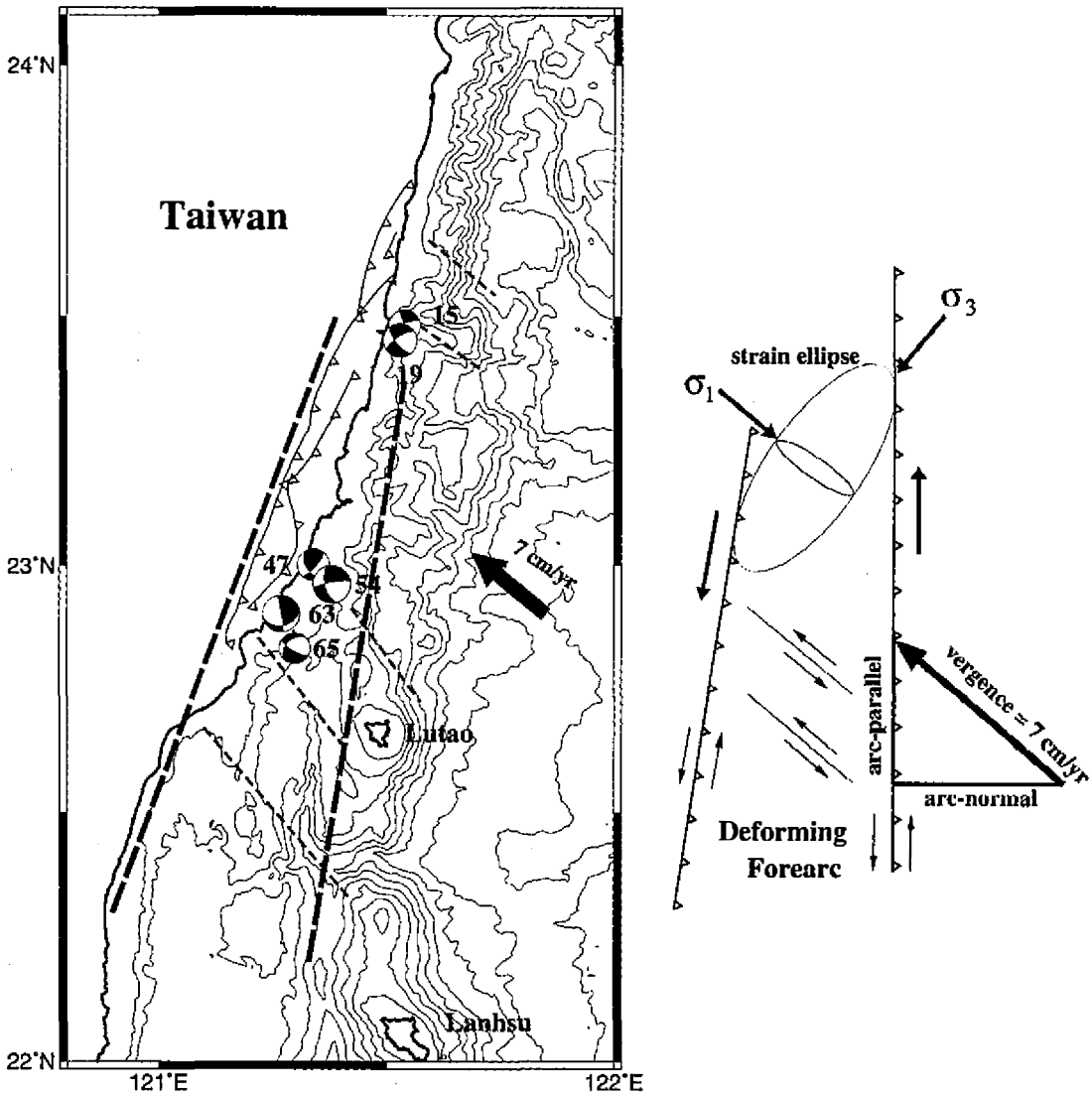
Fig. 6. Schematic diagram showing the Luzon forearc deformation. Left shows
several strike-slip solutions inside the Luzon forearc obtained in this study.
Heavy dashed lines represent roughly the east and west boundaries of the
forearc. Thin dashed lines indicate active strike-slip faults observed in
reflection data (e.g., Fuh et al. 1997; Lallemand et al. 1999; Malavieille
et al. 1999). Right figure shows transpressional model for the Luzon
forearc block. Note the strike-slip faults inside the forearc block also
develop or coincide with thrust faults occurring on both sides.

along the Luzon forearc deformation zone and generation of a stress field with NE-SW extension. During sinistral deformation, σ_1 and σ_3 lay in the horizontal plane, oriented approximately NW-SE and NE-SW respectively, and σ_2 is vertical. In Fig. 6, the Central Range and Luzon arc units represent relatively rigid blocks for the upper crust, which has also been proposed by seismic tomographic study in southeastern Taiwan (Cheng et al. 1998).

We know that the existence of a stress field in the lithosphere is the result of the interaction of tectonic forces whose magnitude and direction vary extremely slowly. Moreover, earthquakes are mostly related to already existing faults, or fault systems in the lithosphere, and these serve as stress concentrators. The forearc unit represents a deforming zone between the two rigid blocks that undergoes simple shearing from the transcurrent component of oblique collision (Fig. 6). The typical effects should occur, such as the formation of en-echelon fold and thrust belts and extensional features that parallel the directions of minimum and maximum compression (e.g., Teyssier et al. 1995). The existence of tensile fracture in a fault system can play an important role because the strike slip displacement can take place not only along the primary faults, but also along the planes of tensile fractures (e.g., Špičák, and Lokajíček, 1986). In addition, strike-slip faults, might also develop or coincide with thrust faults (Sanderson and Marchini 1984). The oblique fold and fault systems of the Coastal Range (left in Fig. 6) and the APSZ and LVSZ in eastern Taiwan could be explained with this model (right in Fig. 6).

6. CONCLUDING REMARKS

Knowledge of the state of stress in the convergent plate boundary is an important constraint on our understanding on seismic and aseismic faulting, the force of resisting plate motion, and the rheology of the crust. To better understand the nature of the seismogenic zone in eastern Taiwan and crustal deformation, focal mechanisms of 70 relocated events generally shallower than 30 km have been determined using P-wave first motion polarity data. The geographical distribution of such events has allowed us to map the seismic strain field of the seismogenic zones in eastern Taiwan. In general, focal mechanisms of events located in the arc-parallel seismic zone (APSZ) and the Longitudinal Valley seismic zone (LVSZ) show mainly thrust and strike-slip solutions in the area south of 23.2°N.

The P-axes for events in both the APSZ and LVSZ are generally oriented in the direction of plate convergence, suggesting some degree of coupling of the plate interface at this depth. However, the orientation of the T-axes indicates that there are different patterns for the APSZ and LVSZ in eastern Taiwan. We infer that these two seismic zones might mark east and west boundaries of the Luzon forearc.

We have developed a transpressional model to explain important tectonic features of the Luzon forearc. Our tectonic model illustrates the pervasive effects of oblique collision processes, combined with subsequent transpressive forces generated by the motion of the forearc sliver parallel to the continental margin. This model suggests that the Luzon forearc deformation plays an important role in accommodating the oblique convergence in eastern Taiwan.

REFERENCES

Angelier, J., H. T. Chu, and J. C. Lee, 1995: Shear concentration in a collision zone: kinematics of the active Chihshang Fault, Longitudinal Valley, eastern Taiwan. In: H. H. Tsien (Ed.), ACT Int. Conf., Ext. Abstr. Geol. Soc. China Spec. Publ., Taipei, pp. 17-24.

Angelier, J., H. T. Chu, J. C., and Lee, 1997: Shear concentration in a collision zone: kinematics of the Chihshang Fault as revealed by outcrop-scale quantification of active faulting, Longitudinal Valley, eastern Taiwan. *Tectonophysics*, **274**, 117-143.

Barrier, E., and J. Angelier, 1986, Active collision in eastern Taiwan: the Coastal Range. *Tectonophysics*, **125**, 39-72.

Bowin, C., R. S. Lu, C. S. Lee, and H. Schouten, 1978: Plate convergence and accretion in the Taiwan-Luzon region. *Am. Assoc. Petro. Geol. Bull.*, **62**, 1645-1672.

Byrne, T., and D. Fisher, 1990: Evidence for a weak and overpressured decollement beneath sediment-dominated accretionary prisms. *J. Geophys. Res.*, **95**, 9081-9097.

Chemenda, A. I., R. K. Yang, C. H. Hsieh, and A. L. Groholsky, 1997: Evolutionary model for the Taiwan collision based on physical modeling. *Tectonophysics*, **274**, 253-274.

Chen, M. -P., and W. S. Juang, 1986: Seafloor physiography off southeastern Taiwan. *Acta Oceanogr. Taiwanica*, **16**, 1-7.

Cheng, S. N., 1995: The study of stress distribution in and around Taiwan [Ph. D. dissert]. Chung-Li, Taiwan, National Central University, 215 p. (in Chinese)

Cheng, W. B., C. Wang, C. T. Shyu, and T. C. Shin, 1998: A three-dimensional Vp model of the southeastern Taiwan area and its tectonic implications. *TAO*, **9**, 425-452.

Cheng, W. B., C. Wang, C. T. Shyu, and T. C. Shin, 1999: Crustal structure of the convergent plate-boundary zone, eastern Taiwan, assessed by seismic tomography. *Geol. Soc. Am. Spec.* (in press)

Dahlen, F. A., J. Suppe, and D. M. Davis, 1984: Mechanics of fold-and thrust belts and accretionary wedges: Cohesive Coulomb theory. *J. Geophys. Res.*, **89**, 10087-10101.

Fuh, S. C., C. S. Liu, N. Lundberg, and D. L. Reed, 1997: Strike-slip faults offshore southern Taiwan: implications for the oblique arc-continent collision processes. *Tectonophysics*, **274**, 25-39.

Ho, C., 1982: Tectonic Evolution of Taiwan. Explanatory Text of the Tectonic Map of Taiwan. Ministry of Economic Affairs, Taipei, 126 pp.

Ho, C., 1986: A synthesis of the geologic evolution of Taiwan. *Tectonophysics*, 125, 1-16.

Hsu, T. L., 1962: Recent faulting in the Longitudinal Valley of eastern Taiwan. *Mem. Geol. Soc. China*, 1, 95-102.

Kao, H., P. R. Jian, K. F. Ma, B. S. Huang, and C. S. Liu, 1998: Moment-tensor inversion of offshore earthquakes east of Taiwan and their implications to regional collision. *Geophys. Res. Lett.*, **25**, 3619-3622.

Kao, H., G. C., Huang, and C. S. Liu, 2000: Transition from oblique subduction to collision in the northern Luzon arc-Taiwan region, Constraints from bathymetry and seismic observations. *J. Geophys. Res.*, **105**, 3059-3079.

Lallemand, S., C. S. Liu, J. Malavielle, P. Schnurle, S. Dominguez, and the ACT scientific crew, 1999: Trench-parallel stretching and folding of forearc basins and lateral migration of the accretionary wedge in the southern Ryukyus: a case of strain partition caused by oblique convergence. *Tectonics*, **18**, 231-247.

Lee, T. Q., C. Kissel, E. Barrier, C. Laj, and W. R. Chi, 1991: Paleomagnetic evidence for a diachronous clockwise rotation of the Coastal Range, eastern Taiwan. *Earth Planet. Sci. Lett.*, **104**, 245-257.

Liu, S. -Y., C. S. Liu, D. Reed, and N. Lundberg, 1992: Analysis of the tectonic structures in the region off southeastern Taiwan based on gravity-magnetic data. *Proc. Taiwan Symposium on Geophys.*, 4th: Taipei, Taiwan, p. 575-585.

Lundberg, N., D. L. Reed, C. S. Liu. and J. Lieske Jr., 1997: Forearc-basin closure and arc accreation in submarine suture zone south of Taiwan. *Tectonophysics*, **274**, 5-23.

Malavieille, J., S. E. Lallemand, S. Dominguez, A. Deschamps, C. Y. Lu, C. S. Liu, P. Schnurle, and the ACT Scientific Crew, 1999: Arc-continent collision in Taiwan: new marine observations and tectonic evolution. *Geol. Soc. Am. Spec.* (in press)

McCaffrey, R., 1992: Oblique plate convergence, slip vectors, and forearc deformation. *J. Geophys. Res.*, **97**, 8905-8915.

McCaffrey, R., 1994: Global variability in subduction thrust zone forearc systems. *Pure App. Geophys.*, **142**, 173-224.

Page, B. M., and J. Suppe, 1981: The Pliocene Lichi Melange of Taiwan: its plate tectonic and olistostromal origin. *Am. J. Science*, **281**, 193-277.

Platt, J. P., 1993: Mechanics of oblique convergence. J. Geophys. Res., 98, 16239-16256.

Reasenberg, P., and D. Oppenheimer, 1985, FPFIT, FPPLOT and FPPAGE: FORTRAN computer programs for calculating and displaying earthquake fault-plane solutions: USGS Open file Rept, 87-739.

Richard, M., H. Bellon, R. C. Maury, E. Barrier, and W. S. Juang, 1986: Miocene to recent calc-alkalic volcanism in eastern Taiwan: K-Ar ages and petrography. *Tectonophysics*, **125**, 87-102.

Sanderson, D., and R. D. Marchini, 1984: Transpression. *J. Struct. Geol.*, **6**, 449-458.

Seno, T., 1977: The instantaneous rotation vector of the Philippine Sea plate relative to the Eurasian plate. *Tectonophysics*, **42**, 209-226.

Shyu, C. T., M. C. Chih, S. K. Hsu, C. Wang, and B. Karp, 1996: Northern Luzon arc: location and tectonic features from magnetic data off eastern Taiwan. *TAO*, **7**, 535-548.

Špičák, A., and T. Lokajíček, 1986: Fault interaction and seismicity: laboratory investigation and its seismotectonic interpretation. *Pure Appl. Geophys.*, **124**, 857-874.

Teyssier, C. B. Tikoff, and M. Markley, 1995: Oblique plate motion and continental tectonics. *Geology*, **23**, 447-450.

Thurber, C. H., 1993: Local earthquake tomography: Velocities and V_p/V_s - Theory, in Iyer, H. M., and Hirahara, K., ed., Seismic Tomography: Theory and Practice: Chapman and Hall, New York, 563-583.

Thurber, C., and D. Eberhart-Phillips, 2000: Local earthquake tomography with flexible gridding. *Computer & Geosciences*, **25**, 809-818.

Tsai, Y. B., 1986: Seismotectonics of Taiwan. *Tectonophysics*, **125**, 17-37

Yu, S. B., H. Y. Chen, and L. C. Kuo, 1997: Velocity field of GPS stations in the Taiwan area. *Tectonophysics*, **274**, 41-59.